Distributed Antenna Systems used for Indoor UE to Access Point Communications at 60 GHz

Yoo, S. K., Zhang, L., Cotton, S. & Ngo, H.

Original citation & hyperlink:
Yoo, SK, Zhang, L, Cotton, S & Ngo, H 2019, Distributed Antenna Systems used for Indoor UE to Access Point Communications at 60 GHz. in 2019 13th European Conference on Antennas and Propagation (EuCAP). IEEE, 13th European Conference on Antennas and Propagation , Krakow, Poland, 31/03/19.

ISBN 9788890701887

Publisher: IEEE

Distributed Antenna Systems used for Indoor UE to Access Point Communications at 60 GHz

Seong Ki Yoo, Lei Zhang, Simon L. Cotton and Hien Quoc Ngo
Centre for Wireless Innovation, ECIT Institute
Queen's University Belfast, BT3 9DT, UK
{sk.yoo, lzhang27, simon.cotton, hien.ngo}@qub.ac.uk

***Abstract*—This paper empirically investigates the performance of distributed antenna systems (DAS) based on switched diversity combining for indoor user equipment (UE) to access point (AP) communications at 60 GHz. Among the candidate pool of switched diversity combining techniques, the pure selection combining (PSC), switch-and-examine combining (SEC) and SEC with post-examining selection (SECps) schemes are utilized to combine the received composite fading signals. Unlike the PSC scheme, the performance and complexity of the SEC and SECps schemes vary according to the switching threshold that is used, highlighting the importance of the selection of an appropriate switching threshold level. Also in this study, diversity specific equations are developed under the assumption of independent and identically distributed F composite fading channels. These are then utilized to model the composite fading behavior observed at the output of each of the combiners. Over all of the measurement scenarios considered in this study, it is found that the theoretical models provided an adequate fit to the composite fading observed at the output of each of the combiners.**

***Index Terms*—Channel measurement, F composite fading, millimeter-wave, switched diversity.**

I. Introduction

Millimeter-wave (mmWave) frequency bands will play an increasingly important role in wireless networks, driven in part to satisfy the demand for higher data rates [1]. Within the mmWave frequency bands, the unlicensed 60 GHz band is particularly attractive as it contains approximately 7 GHz of spectrum worldwide, providing the potential to develop wireless communication systems with multi-gigabit throughput. In this respect, the 60 GHz band has been proposed as a promising candidate for multi-gigabit short range indoor wireless communications [2], which are an important part of the next generation wireless local area networks (WLANs) and wireless personal area networks (WPANs).

For short range mmWave communications, the availability of a line-of-sight (LOS) link between the user equipment (UE) and access point (AP), or equivalently evolved NodeB in the case of cellular communications systems, is not always guaranteed. This is mainly due to the high susceptibility of mmWave links to the shadowing (or equivalently signal blockage) caused by different obstacles which may be present in the local environment [3], [4]. In particular, for UE usage cases where wireless devices are operated in close proximity to the user's body while the user is mobile, shadowing effects can be prevalent [3]. These effects can significantly impact the performance of mmWave wireless systems by introducing deep and often prolonged shadowed fading events.

One possible method to lessen the intensity of these shadowed fading events is to utilize macro diversity by deploying multiple base stations (or equivalently APs as used in this study). Two different categories of combining are typically employed to combine the signals received at multiple spatially separated base stations, namely switched combining and gain combining [5]. In the former grouping, the receiver selects one of the available diversity paths according to a corresponding criterion. On the other hand, in the latter grouping, the output of combiner is formed as a linear combination of the signals received by all of the diversity paths. In general, gain combining provides a better performance compared to switched combining. Nevertheless, switched combining has remained popular due to its relatively low complexity and ease of implementation.

Therefore, in this study, we examine the possible signal reliability improvement for indoor UE-to-AP communications channels operating at 60 GHz using distributed antenna systems (DAS) in conjunction with three different switched combining techniques, namely pure selection combining (PSC), switch-and-examine combining (SEC), and SEC with post-examining selection (SECps) schemes. Notably, we perform an important empirical investigation of the achievable diversity gain (performance) and number of path examinations (complexity) for the PSC, SEC and SECps schemes. Following from this, we statistically characterize the composite fading behavior observed at the output of each switched diversity combiners, i.e., from the perspective of the combiner output, using the diversity specific equations which were developed under the assumption of independent and identically distributed (i.i.d.) F composite fading channels.

The remainder of the paper is organized as follows. In Section II, we briefly review the characteristics of the F composite fading model before introducing theoretical equations for the probability density functions (PDFs) of L-branch PSC, L-branch SEC and L-branch SECps operating in i.i.d. F composite fading channels. In Section III, the experimental setup and measurement procedure are described. In Section IV, diversity gain and the number of path examinations for the considered diversity combiners are presented in conjunction with some examples of the model fitting. Finally, we conclude this study with some closing remarks in Section V.

II. Spatial Diversity Systems Operating in F Composite Fading Channels

A. F Composite Fading Model

There have been a number of different models used to describe the statistical behavior of composite fading experienced in mobile radio propagation channels [6–8]. Among them, the F composite fading model has recently received much attention as it provides as good and in most cases better fit to real-world composite fading channels compared to other models proposed in the literature [8]. Moreover, the key statistical metrics and performance measures of the F composite fading model show low complexity. The corresponding PDF and cumulative distribution function (CDF) of the received signal envelope in an F fading channel can be expressed as

$$f_R(r) = \frac{2\, m^m (m_s - 1)^{m_s} \Omega^{m_s} r^{2m-1}}{B\left(m, m_s\right) \left(m r^2 + (m_s - 1)\,\Omega\right)^{m+m_s}}, m_s > 1 \quad (1)$$

and

$$F_R(r) = \frac{m^{m-1} r^{2m} {}_2F_1\left(m + m_s, m; m+1; -\dfrac{m r^2}{(m_s-1)\Omega}\right)}{B\left(m, m_s\right) \left(m_s\, - 1\right)^m \Omega^m} \quad (2)$$

where $B(\cdot, \cdot)$ and ${}_2F_1(\cdot, \cdot; \cdot; \cdot)$ denote the beta function [9, eq. (8.384.1)] and the Gauss hypergeometric function [9, eq. (9.111)], respectively. In this model, m and m_s represent the fading and shadowing severity parameters, respectively. Moreover, $\Omega = \mathbb{E}[r^2]$ is the mean signal power with $\mathbb{E}[\cdot]$ denoting the statistical expectation.

B. L-branch PSC over F Composite Fading Channels

In a PSC scheme, the combiner monitors the input signal level of all the diversity paths simultaneously and selects the branch with the highest signal level, i.e., $r_{PSC} = \max\{r_1, r_2, \ldots, r_L\}$ where r_L is the signal observed at the L^{th} branch of the diversity receiver. For L-branch PSC system in which the input envelope is i.i.d. at each of the L branches, the PDF of the output envelope can be obtained as [10]

$$f_R^{PSC}(r) = L \left[F_R(r)\right]^{L-1} f_R(r). \quad (3)$$

To obtain the PDF of the output envelope of an L-branch PSC system operating i.i.d. F composite fading channels, we can simply substitute (1) and (2) into (3). After some algebraic manipulations, we arrive at the expression given in (4) at the top of the next page.

C. L-Branch SEC over F Composite Fading Channels

With an SEC scheme, the receiver switches to an alternative branch and examines its input signal level. If it is not above the predetermined threshold, the receiver switches to an alternative branch and examines the input signal level again. This process continues until the receiver either finds an acceptable branch or determines that no acceptable branch is available. In the latter case, the receiver usually selects the last branch that was examined. For an SEC scheme, when the input signal level of the current branch falls below the switching threshold, path switching between branches always happens regardless of whether the input signal level of another branch is above or below that of the current branch. In fact, in the latter case, path switching can degrade the system performance.

For an L-branch SEC system in which the input envelope is i.i.d. at each of the L branches, the PDF of the output envelope, R, can be expressed as [11]

$$f_R^{SEC}(r) = \begin{cases} F_R\left(r_T\right)^{L-1} f_R(r), & r < r_T \\ \sum\limits_{i=0}^{L-1} \left[F_R\left(r_T\right)\right]^i f_R(r), & r \geq r_T \end{cases} \quad (5)$$

where r_T is the predetermined switching threshold. Similarly, the PDF of the output envelope of an L-branch SEC combiner operating in an F fading environment can be obtained by substituting (1) and (2) into (5) and performing some algebraic manipulations to yield (6) as shown at the top of the next page.

D. L-Branch SECps over F Composite Fading Channels

A receiver employing an SECps scheme works in exactly the same manner as an SEC scheme when an acceptable branch is available. However, when there is no acceptable branch available, the receiver selects the branch with the highest signal level (in the same manner as a PSC scheme) instead of the previously examined one. Consequently, for an L-branch SECps system in which the input envelope is i.i.d. at each of the L branches, the PDF of the output envelope, R, can be expressed with the aid of (3) and (5), such that [11]

$$f_R^{SECps}(r) = \begin{cases} L\left[F_R(r)\right]^{L-1} f_R(r), & r < r_T \\ \sum\limits_{i=0}^{L-1} \left[F_R\left(r_T\right)\right]^i f_R(r), & r \geq r_T. \end{cases} \quad (7)$$

Again, the PDF of the output envelope of an L-branch SECps combiner operating in an F composite fading environment can be obtained by substituting (1) and (2) into (7) and then performing some algebraic manipulations to give (8) as shown at the top of the next page.

III. Experimental Setup and Measurements

A. Experimental Setup

The hypothetical mmWave UE and APs used for the 60 GHz measurements consisted of a Hittite HMC6000LP711E transmitter (TX)[1] and Hittite HMC6001LP711E receiver (RX)[2] modules, respectively. Both the TX and RX modules featured on-chip low profile antennas with +7.5 dBi gain. For the mmWave UE, a CW tone of 50 MHz baseband frequency was fed into a 90° splitter to provide the analogue baseband I/Q signal. This configuration enabled us to transmit a narrowband signal centered at 60.05 GHz using at an Equivalent Isotropically Radiated Power (EIRP) of +10.9 dBm. For the mmWave APs, the 50 MHz intermediate frequency (IF) signal outputted by the RX module was sampled using a v1.4 Red

[1] http://www.analog.com/media/en/technical-documentation/data-sheets/hmc6000.pdf (visited on 10/12/2018).

[2] http://www.analog.com/media/en/technical-documentation/data-sheets/hmc6001.pdf (visited on 10/12/2018).

$$f_R^{PSC}(r) = \frac{2L\, m^{mL-L+1}((m_s-1)\Omega)^{m_s-mL+m} r^{2mL-1}}{[B(m,m_s)]^L (mr^2+(m_s-1)\Omega)^{m+m_s}} \left[{}_2F_1 \left(m+m_s, m; m+1; -\frac{mr^2}{(m_s-1)\,\Omega} \right) \right]^{L-1} \tag{4}$$

$$f_R^{SEC}(r) = \begin{cases} \dfrac{2\, m^{mL-L+1}\,((m_s-1)\Omega)^{m_s-mL+m} r_T^{2m(L-1)} r^{2m-1}}{[B(m,m_s)]^L (mr^2+(m_s-1)\Omega)^{m+m_s}} \left[{}_2F_1 \left(m+m_s, m; m+1; -\dfrac{mr_T^2}{(m_s-1)\,\Omega} \right) \right]^{L-1}, & r < r_T \\ \displaystyle\sum_{i=0}^{L-1} \dfrac{2\, m^{(m-1)i+m}\,((m_s-1)\Omega)^{m_s-mi}\, r_T^{2mi}\, r^{2m-1}}{[B(m,m_s)]^{i+1} (mr^2+(m_s-1)\Omega)^{m+m_s}} \left[{}_2F_1 \left(m+m_s, m; m+1; -\dfrac{mr_T^2}{(m_s-1)\,\Omega} \right) \right]^{i}, & r \geq r_T \end{cases} \tag{6}$$

$$f_R^{SECps}(r) = \begin{cases} \dfrac{2L\, m^{mL-L+1}((m_s-1)\Omega)^{m_s-mL+m} r^{2mL-1}}{[B(m,m_s)]^L (mr^2+(m_s-1)\Omega)^{m+m_s}} \left[{}_2F_1 \left(m+m_s, m; m+1; -\dfrac{mr^2}{(m_s-1)\,\Omega} \right) \right]^{L-1}, & r < r_T \\ \displaystyle\sum_{i=0}^{L-1} \dfrac{2\, m^{(m-1)i+m}\,((m_s-1)\Omega)^{m_s-mi}\, r_T^{2mi}\, r^{2m-1}}{[B(m,m_s)]^{i+1} (mr^2+(m_s-1)\Omega)^{m+m_s}} \left[{}_2F_1 \left(m+m_s, m; m+1; -\dfrac{mr_T^2}{(m_s-1)\,\Omega} \right) \right]^{i}, & r \geq r_T \end{cases} \tag{8}$$

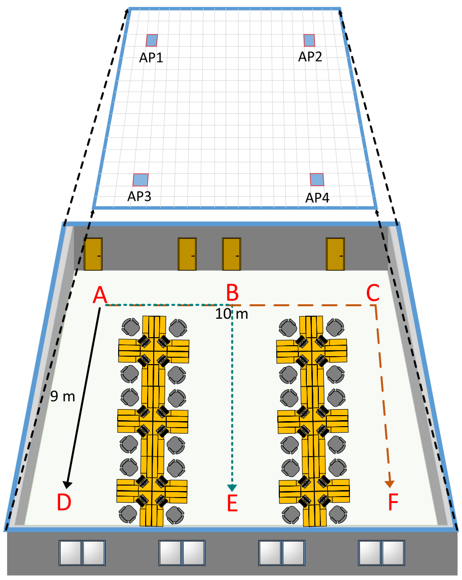

Fig. 1. Open office environment showing the positions of the APs and user trajectories.

Pitaya data acquisition platform. The Red Pitaya v1.4 contains a 14-bit, 125 Msps analog-to-digital converter (ADC) which was connected to a field programmable gate array (FPGA). The FPGA unit was programmed with a custom direct digital down conversion implementation based on the embedded SDR receiver described in [12]. This implementation provided an effective channel sampling frequency of 2 kHz and a receive bandwidth of 86 kHz.

B. *Measurement Environment and Scenarios*

The measurements were conducted in an indoor open office area as shown in Fig. 1, which is situated on the 1st floor of the Institute of Electronics, Communications and Information Technology (ECIT) at Queen's University Belfast in the United Kingdom. The indoor environment featured metal studded dry walls with a metal tiled floor covered with polypropylene-fiber, rubber backed carpet tiles, and metal ceiling with mineral fiber tiles and recessed louvered luminaries suspended 2.70 m above floor level. The open office area was unoccupied for the duration of the measurements. As shown in Fig. 1, the hypothetical DAS array consisted of four identical APs, which were positioned in a rectangular configuration with a length of 10.0 m and a width of 9.0 m. It is worth remarking that the mmWave APs were placed above the ceiling tile with the antenna boresight oriented towards the floor. During the measurements, an adult male of height of 1.83 m and mass 80 kg imitated operating an app where the user held the UE with his right hand in front of his body. The user walked along three different paths, namely *paths AD*, *ABE* and *ACF* (Fig. 1).

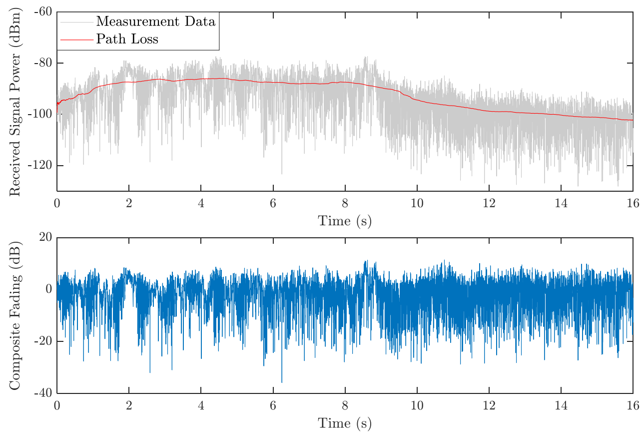

Fig. 2. Received signal power (gray continuous lines) measured at AP2 with the path loss component (red continuous lines) alongside the extracted composite fading component (blue continuous lines) for the *path ACF*.

IV. Results

A. *Diversity Gain and Number of Path Examinations*

As shown in Fig. 2, using the approach described in [13], the composite fading signal was firstly extracted from the

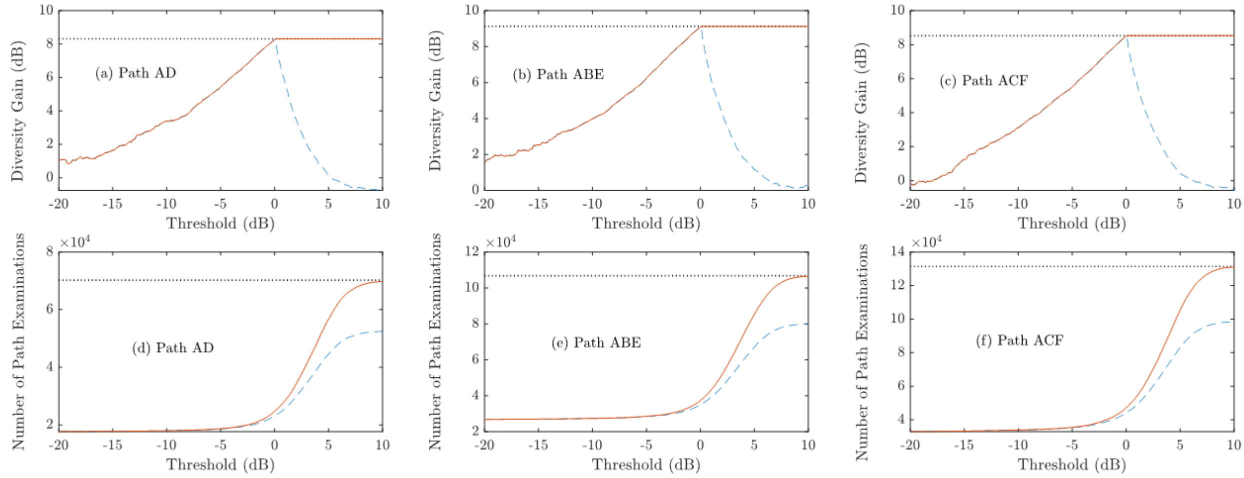

Fig. 3. (a)-(c) Diversity gain and (d)-(f) the number of path examinations for the PSC (black dotted lines), SEC (blue dashed lines) and SECps (red continuous lines) schemes for all walking scenarios.

measurement data by removing the estimated path loss.[3] Then, the concept of diversity gain was utilized to evaluate the potential improvement in the received composite fading signal reliability that could be obtained using the DAS arrangement along with the PSC, SEC and SECps schemes. The diversity gain is defined as the improvement in the signal reliability of a diversity combiner over the target AP for a given probability or signal reliability.[4] It is remarking that all diversity gain calculations were made at a cumulative probability of 0.1 (10% CDF level) which is equivalent to a signal reliability of 90%.

Figs. 3(a)-(c) show the achievable diversity gain statistics for all of the walking paths and the four AP DAS system. It is clear that the diversity gain of the SEC and SECps schemes strongly depends on the predetermined switching threshold and there exists an optimum switching threshold that maximizes the diversity gain. It was also observed that the diversity gain obtained for the SEC and SECps schemes when using the optimum switching threshold was almost the same as the one for the PSC scheme. In contrast with the SEC scheme, the diversity gain for the SECps scheme kept the same diversity gain beyond the optimum switching threshold.

As shown in Figs. 3(d)-(f), the number of path examinations for the PSC, SEC and SECps schemes was also computed to evaluate their complexity. Although the number of path examinations increases as the switching threshold level increases, the SEC and SECps schemes still had a smaller number of path examinations compared to the PSC scheme for the majority of switching threshold levels. Moreover, the number of path examinations for the SEC and SECps schemes were almost the same when the switching threshold is less than 0 dB while the SECps scheme had a greater number of path examinations compared to the SEC scheme when the switching threshold is greater than 0 dB. This was most likely due to the fact that when there is no acceptable branch available the SEC scheme usually selects the last examined branch while the SECps scheme selects the best performing branch. More specifically, for an L-branch arrangement, when the receiver switches from the $(L-1)^{\text{th}}$ branch to the L^{th} branch (i.e., last branch), the SECps scheme needs to monitor the L^{th} branch whereas the SEC scheme does not need to do this as it switches to the L^{th} branch anyway irrespective of whether the received signal level at the L^{th} branch is above the switching threshold or not.

B. Modeling of the Composite Fading Behavior Observed at the Combiner Output

The modeling of the composite fading characteristics observed at the output of the hypothetical combiners considered in this paper was performed using the diversity specific equations presented in Section II. The m, m_s and Ω parameters were estimated using a nonlinear least squares routine programmed in MATLAB to fit (4), (6), and (8) to the measurement data. Table I shows the respective parameter estimates for all of the considered walking paths, allowing the reader to reproduce their own simulated data based on the empirical measurements reported here. It is clear that the m_s parameters were found to be quite large for many of the scenarios, suggesting that they could be approximated using the equivalent Nakagami-m expressions [15].

As an example of the results of the model fitting process, Fig. 4 shows the PDFs of the PSC, SEC and SECps schemes fitted to the measurement data for the *path ACF*. It is worth highlighting that the switching threshold was 0 dB. The theoretical PDFs of the PSC, SEC and SECps schemes were in very good agreement with the measured composite fading at the output of each of the combiners, confirming the validity of the modeling approach utilized here. It can also be seen that the majority of the composite fading signal levels observed at the output of the PSC and SECps schemes ranged between -10 dB and 10 dB while the SEC scheme still had instances

[3] In our analysis, we assume that the APs employ a power control scheme (e.g., fractional power control [14]) to compensate for the attenuation due to the path loss.

[4] In this study, the target AP was chosen in post-processing as the AP with the highest mean.

TABLE I
PARAMETER ESTIMATES FOR THE PSC, SEC AND SECPS SCHEMES FOR ALL OF THE CONSIDERED WALKING PATHS

Walking Path	PSC			SEC			SECps		
	m	Ω	m_s	m	Ω	m_s	m	Ω	m_s
Path AD	1.10	1.25	22.62	0.92	1.39	129.99	0.86	1.33	130.00
Path ABE	1.11	1.26	17.82	0.95	1.42	130.00	0.89	1.40	129.99
Path ACF	1.01	1.24	130.00	0.93	1.39	129.99	0.88	1.34	130.00

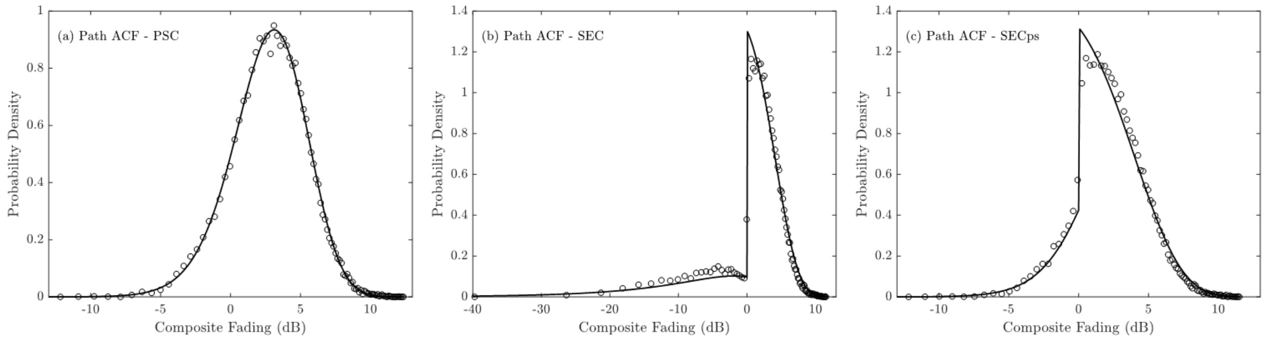

Fig. 4. Empirical PDFs (circles) of the composite fading signal observed at the output of (a) PSC; (b) SEC; (c) SECps schemes for the *path ACF* compared to the corresponding theoretical PDFs (continuous lines). It is worth highlighting that the switching threshold was 0 dB.

where the composite fading level was below -10 dB.

V. CONCLUSION

In this paper, the potential improvement in the received composite fading signal for indoor mmWave UE-to-AP communications using DAS based on PSC, SEC and SECps schemes has been investigated in terms of the achievable diversity gain. It has been shown that all the considered diversity schemes provided a worthwhile signal improvement (up to 9.1 dB of the diversity gain) although the diversity gain for the SEC and SECps schemes varied according to the switching threshold that was used. Following this, their complexity has also been evaluated in terms of the number of path examinations. When compared to the PSC scheme, and using an appropriate switching threshold level, the SEC and SECps schemes provided a similar performance with less complexity by preventing the unnecessary monitoring. Finally, a statistical analysis of the output envelope of the PSC, SEC and SECps schemes operating in i.i.d. F composite fading channels has been presented. Over all of the experimental scenarios considered in this study, the PDFs of the switched diversity combiners have been shown to provide an adequate fit to the composite fading observed at the output of the virtual switched diversity combiners.

ACKNOWLEDGMENT

This work was supported by the Engineering and Physical Sciences Research Council under Grant Reference EP/L026074/1 and the Department for Employment and Learning Northern Ireland through Grant Reference USI080.

REFERENCES

[1] S. Rangan, T. S. Rappaport, and E. Erkip, "Millimeter-wave cellular wireless networks: Potentials and challenges," *Proc. IEEE*, vol. 102, no. 3, pp. 366–385, Mar. 2014.

[2] C. Park and T. S. Rappaport, "Short-range wireless communications for next-generation networks: UWB, 60 GHz millimeter-wave WPAN, and ZigBee," *IEEE Wireless Commun.*, vol. 14, no. 4, Aug. 2007.

[3] S. K. Yoo, S. L. Cotton, R. W. Heath, and Y. J. Chun, "Measurements of the 60 GHz UE to eNB channel for small cell deployments," *IEEE Wireless Commun. Lett.*, vol. 6, no. 2, pp. 178–181, Apr. 2017.

[4] S. Singh, F. Ziliotto, U. Madhow, E. Belding, and M. Rodwell, "Blockage and directivity in 60 GHz wireless personal area networks: From cross-layer model to multihop MAC design," *IIEEE J. Select. Areas Commun.*, vol. 27, no. 8, Oct. 2009.

[5] M. D. Yacoub, *Foundations of mobile radio engineering*. CRC press, 1993.

[6] I. M. Kostić, "Analytical approach to performance analysis for channel subject to shadowing and fading," *IEE Proc. Comm.*, vol. 152, no. 6, pp. 821–827, Dec. 2005.

[7] A. Abdi and M. Kaveh, "K distribution: An appropriate substitute for Rayleigh-lognormal distribution in fading-shadowing wireless channels," *IET Electron. Lett.*, vol. 34, no. 9, pp. 851–852, Apr. 1998.

[8] S. K. Yoo, S. Cotton, P. Sofotasios, M. Matthaiou, M. Valkama, and G. Karagiannidis, "The Fisher-Snedecor $\mathcal{F}$ distribution: A simple and accurate composite fading model," *IEEE Commun. Lett.*, vol. 21, no. 7, pp. 1661–1664, Jul. 2017.

[9] I. S. Gradshteyn and I. M. Ryzhik, *Table of Integrals, Series, and Products*, 7th ed. London: Academic Press, 2007.

[10] M. D. Yacoub, C. R. C. M. da Silva, and J. V. Bautista, "Second-order statistics for diversity-combining techniques in Nakagami-fading channels," *IEEE Trans. Veh. Technol.*, vol. 50, no. 6, pp. 1464–1470, 2001.

[11] H.-C. Yang and M.-S. Alouini, "Performance analysis of multibranch switched diversity systems," *IEEE Trans. Commun.*, vol. 51, no. 5, pp. 782–794, May 2003.

[12] Red Pitaya Notes, visited on 10/12/2018. [Online]. Available: http://pavel-demin.github.io/red-pitaya-notes/.

[13] N. Jaldén, P. Zetterberg, B. Ottersten, A. Hong, and R. Thoma, "Correlation properties of large scale fading based on indoor measurements," in *Proc. WCNC*, Mar. 2007, pp. 1894–1899.

[14] S. Essassi, M. Siala, and S. Cherif, "Dynamic fractional power control for LTE uplink," in *Proc. IEEE PIMRC*, Sep. 2011, pp. 1606–1610.

[15] S. K. Yoo, S. L. Cotton, and W. G. Scanlon, "Switched diversity techniques for indoor off-body communication channels: An experimental analysis and modeling," *IEEE Trans. Antennas Propag.,*, vol. 64, no. 7, pp. 3201–3206, Jul. 2017.